# "STRUCTURE BASED DRUG DESIGN, SYNTHESIS AND BIOLOGICAL EVALUATIONOF (E)-4-($ CHLOROBENZYLIDENEAMINO)-6-PHENYL-3-THIOXO-3,4-DIHYDRO -1,2,4- TRIAZIN-5(2H)-ONE DERIVATIVES AS DYRK1A, CLK1A,GSK INHIBITORS"

Ravindra mishra[1]*, Anoop singh[2]*

1, Research scholar, Department of pharmacy, Bhagwant university ajmer rajasthan india (305001)

2, Department of pharmacy, pharmacy, Bhagwant university ajmer rajasthan india

## Abstract

A sharp increase in the incident of Alzheimer's disease (AD) especially in developed and developing countries is a matter of serious concern. It is predicted that 26 million people are affected by Alzheimer's disease worldwide and it will be triple by the year 2050. There are two groups of drugs available on the market, which are classified according to their mechanism of action Inhibitors of acetyl cholinesterase and NMDA receptor inhibitors have beneficial effects on cognitive, functional, and behavioral symptoms of the disease, but their role in AD pathogenesis is unknown. Current treatments for AD provide only modest symptomatic relief. There is an urgent need for 'disease modifying' agents that slow the course of the disease and prevent or delay the disease in susceptible individuals.

Protein phosphorylation, the most common post-translational mechanism used by cells to regulate enzymes and structural proteins, is controlled by ≈520 protein kinases and ≈80 protein phosphatases. Because many diseases are associated with abnormalities of protein phosphorylation, pharmacological inhibitors of kinases and phosphatases have become a major interest in drug discovery. In AD, aberrant phosphorylation of tau, an alternatively spliced microtubule-binding protein, is believed to contribute to neurodegeneration. Hyperphosphorylation of *tau* leads to loss of normal *tau* functioning and attenuates the stability of neuronal microtubules. In addition, *tau* hyperphosphorylation is also associated with aggregation of the protein into neurofibrillary tangles, contributing to neurofibrillary degeneration, neuronal death, and dementia severity. A plethora of evidence recorded in the literature suggests that targeting tau phosphorylation through inhibition of protein kinases could represent a valid therapeutic approach to reduce *tau* aggregation and associated neuronal death in AD and other neurodegenerative 'taupathies'. Dual specificity tyrosine phosphorylation-regulated kinase 1A (DYRK1A), and human CDC2-like kinase 1 (CLK1) are involved in the key molecular feature of AD, hyperphosphorylation of the microtubule-binding protein Tau (intracellular neurofibrillary tangles)11-13. Consequently, small molecule inhibitors acting on these kinases could be of great therapeutic value in AD and related taupathies. With the abovementioned rationale, the objective of this research is to discover novel lead molecules that are inhibitors of DYRK1A and CLK1 kinase with therapeutical potential in Alzheimer's Disease.

The availability of multiple crystal structures of DYRK1A and CLK1 complexed with inhibitors provides an opportunity for utilizing the structure based high-throughput virtual screening strategy for identifying potent and pharmacologically favorable inhibitors of DYRK1A and CLK1. With this understanding, the present research will employ a docking-based

virtual screening technique to screen a commercially available chemical database against DYRK1A and CLK1 for identification of potent and diverse lead molecules with DYRK1A and CLK1 inhibitory activity. The identified lead molecules will be further optimized through SAR approach to give optimal candidates for translation into the clinic

**Key word -** CLK (casein like kinase), Down syndrome, potential inhibitors, DYRK1A(Dual specificity tyrosine-phosphorylation-regulated kinase 1A)

## Introduction

Down syndrome (DS) was first described in 1866 by British doctor, John L. H. Down. DS is the consequence of trisomy of human chromosome 21 and is the most common genetic form of intellectual disability, occurring in approximately 1 in 700 live births. DS is characterized by learning disabilities, craniofacial abnormalities and hypotonia craniofacial abnormalities, congenital heart defects of the endocardial cushions, clinodactyl of the fifth finger and mental retardation. Those characteristics result from the extra- genes located in the specific region called 'Down syndrome critical region (DSCR)' in human chromosome 21. The additional copy of Hsa21 results in elevated expression of many of the genes encoded on this chromosome, with varying expression levels in different tissues. The increased dosage of Hsa21 genes and the dosage imbalance between Hsa21 and non-Hsa21 genes has been proposed to cause the plethora of phenotypic alterations that characterize DS. The gene-rich distal part of Hsa21, identified as the 'Down syndrome critical region' (DSCR), was initially proposed to be sufficient to cause most of these DS phenotypes. DSeventually leads to development of Alzheimer's disease type pathology (the formation of amyloid plaques and neurofibrillary tangles). In addition, individuals with Down's syndrome exhibit characteristic patterns.

## 1.1Signs and symptoms

The signs and symptoms of Down syndrome are characterized by the neotenization of the brain and body to the fetal state. Individuals with Down syndrome may have some or all of the following physical characteristics are microgenia (abnormally small chin), oblique eye fissures with epicanthic skin folds on the inner corner of the eyes (formerly known as a mongoloid fold), muscle hypotonia (poor muscle tone), a flat nasal bridge, a single palmar fold, a protruding tongue (due to small oral cavity, and an enlarged tongue near the tonsils) or macroglossia,face is flat and broad, a short neck, white spots on the iris known as Brushfield spots, excessive joint laxity including atlanto-axial instability, excessive space between large toe and second toe, a single flexion furrow of the fifth finger, a higher number of ulnar loop dermatoglyphs and short fingers.

## 1.1.1Causes of Down syndrome [1]

Down syndrome occurs because of an abnormality characterized by an extra copy of genetic material on all or part of the 21st chromosome. Every cell in the body contains genes that are grouped along chromosomes in the cell's nucleus or center. There are normally 46 chromosomes in each cell, 23 each from both parents. When some or all of a person's cells have an extra full or partial copy of chromosome 21, the result is DS.
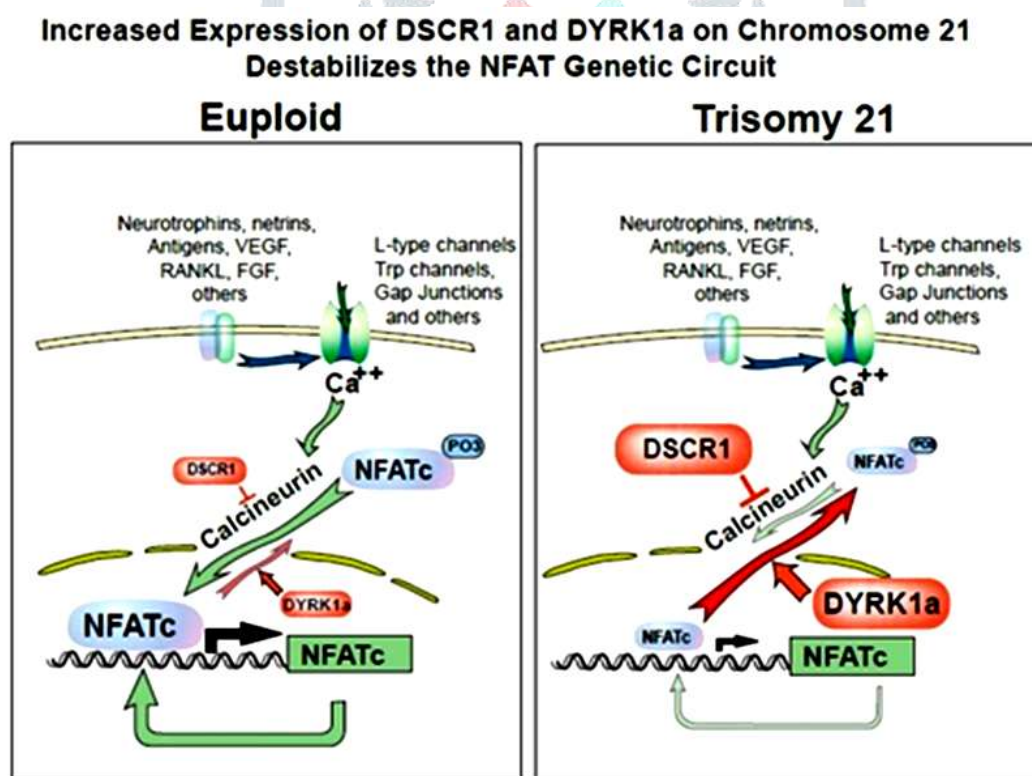
The most common form of DS is known as Trisomy 21, a condition where individual has 47 chromosomes in each cell instead of 46. This is caused by an error in cell division called nondisjunction, which leaves a sperm or egg cell with an extra copy of chromosome 21 before or at conception. Trisomy 21 accounts for 95% of DS cases, with 88% originating from non-disjunction of the mother's egg cell.The remaining 5% of DS cases are

due to conditions called mosaicism and translocation. Mosaic DS results cells in body are both normal as well as a Trisomy of 21. Robertsonian translocation occurs when part of chromosome 21 breaks off during cell division and attaches to another chromosome (usually chromosome 14). The presence of this extra part of chromosome 21 causes down some syndrome characteristics. Although a person with a translocation may appear physically normal, he or she has a greater risk of producing a child with an extra 21 chromosome.

### 1.1.2 NFAT signaling and Down's syndrome[2]

Calcium signaling through the NFAT pathway mediates many developmental processes and the immune response.

A. The entry of calcium ions into the cell activates the enzyme calcineurin to remove phosphate groups (P) from NFATc factors in the cytoplasm, allowing NFATc to enter the nucleus and activate its target genes.

B. However, once in the nucleus, the NFATc can be phosphorylated, and so returns to the cytoplasm. The DSCR1 and DYRK1A proteins in regulating the levels of NFATc phosphorylation.

C. The genes encoding DSCR1 and DYRK1A are found in the 'Down's syndrome critical region' of human chromosome 21, which has an extra copy in people with Down's syndrome. The increased expression of *DSCR1* and *DYRK1A* disturbs the balance of NFATc phosphorylation, so that most of the protein is found in the cytoplasm. Thus, NFATc-dependent genes will not be properly regulated, which could markedly affect development.



**Figure 1.1** *Increased Expressions of DSCR1 and DYRK1A.*

## 1.2 Alzheimer disease[3, 4, 5, 6]

Alzheimer's disease was discovered in 1906 by Alois Alzheimer, a German neurologist and psychiatrist. The disease was initially observed in a 51-year-old woman named Auguste D.Dr. Alzheimer performed an autopsy, during which he found dramatic shrinkage of the cerebral cortex, fatty deposits in blood vessels, and atrophied brain cells. He discovered neurofibrillary tangles and senile plaques which have become indicative of AD. The condition was first discussed in medical literature in 1907 and named after Alzheimer in 1910.

Approximately 35 million people worldwide suffer from Alzheimer's disease (AD), the most common form of dementia, often leading to death within 3 to 9 years of diagnosis. There are 1275 new cases per year per 100, 000 persons over the age of 65, signifying a doubling of the disease incidence every five years. The prevailing hypothesis for the cause of cognitive decline is thought to stem from an increase in soluble amyloid beta (Aβ) oligomers and hyperphosphorylated *Tau*, which coalesces into soluble, paired helical filaments. Aβ production is regulated by beta and gamma secretase proteolytic processing of the amyloid precursor protein (APP).

Alzheimer's disease (AD) is an irreversible, progressive neurodegenerative disorder that occurs gradually and results in memory loss, unusual behaviour, personality changes, and a decline in thinking abilities. In AD, the progressive nature of neurodegeneration suggests an age-dependent process that ultimately leads to degeneration of synaptic afferent systems, dendritic and neuronal damage, and the formation of abnormal protein aggregates throughout the brain. The age-related susceptibility of the brain to neurodegenerative disease may be inherent in the susceptibility of individual neurons to various stressors. The prevalence of AD varies among many different factors, including age, co-morbidities, genetics, and education level. There is no way to definitively diagnose AD without performing an autopsy. There is no cure for AD, however promising research and development for early detection and treatment is underway.

### 1.2.1 Alzheimer's Disease vs. Dementia and Normal Aging[7, 8, 9]

Alzheimer's disease is often confused with normal aging and dementia. Severe memory loss, characteristic of AD, is not a symptom of normal aging. Healthy aging may involve the gradual loss of hair, weight, height and muscle mass. Skin may become more fragile and bone density can be lost. A decrease in hearing and vision may occur, as well as a decrease in metabolic rate. It is common to have a slight decline in memory, such as slower recall of information, however cognitive decline that impacts daily life is not a normal part of the aging process.

Dementia is defined as the significant loss of cognitive abilities severe enough to interfere with social functioning. It can result from various diseases that cause damage to brain cells. There are many different types of dementia, each with its own cause and symptoms.

For example, vascular dementia is caused by decreased blood flow to a part of the brain, as caused by a stroke. Dementia may also be present in patients with Parkinson's disease and hydrocephalus. AD is the most common form of dementia, caused by the build-up of beta amyloid plaques in the brain.

### 1.2.1.1 Characteristics

The disease course is divided into four stages, with progressive patterns of cognitive and functionalimpairments

### 1.2.1.2 Early-Stage Alzheimer's disease[10, 11, 12, 13]

This mild stage, which usually lasts 2 to 4 years, is often when the disease is first diagnosed. In this stage, family and friends may begin to realize that there has been a decline in the patient's cognitive ability. Common symptoms at this stage include;

- Difficulty retaining new information.
- Difficulty with problem solving or decision making. Patients may start to have trouble managing finances or other instrumental activities of daily living.  Personality changes. The person may begin to withdraw socially or show lack of motivation.
- Difficulty expressing thoughts Misplacing belongings or getting lost.
-  The patient may have difficulty navigating in familiar surroundings.

### 1.2.2 Moderate Alzheimer's disease

Lasting 2 to 10 years, this is longest stage of the disease. Patients often experience increased difficulty with memory and may need help with activities of daily living. Symptoms frequently reported during this stage include;

- Increasingly poor judgment and confusion. The patient may begin to confuse family members, lose orientation to time and place, and may begin wandering, making it unsafe for them to be left alone.
-  Difficulty completing complex tasks, including many of the instrumental activities of daily living, such as managing finances, grocery shopping, planning, and organization.
- Greater memory loss. Patients may begin to forget details of their personal history.
- Significant personality changes. The person may become withdrawn from social interactions and develop unusually high suspicions of caregivers.
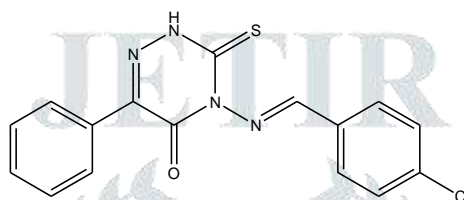
### 2.Objective

A sharp increase in the incident of Alzheimer's disease especially in developed and developing countries is a matter of serious concern. It is predicted that **26 million people are affected by Alzheimer's disease worldwide and it will be triple by the year 2050. The most common form of the disease is that which affects those over 60 years,** and whose incidence rises with age. It is estimated that 24% of the population over 85 is affected by Alzheimer's disease. Alzheimer's disease is more frequent in women and **accounts for more than 65% of dementias in people of advanced age. The duration of the disease ranges between 2 and 20 years, with an average survival period of 10 years.** Current treatment for Alzheimer's disease is **merely symptomatic, offering slight improvements and effective only during a limited period of time.** There are two groups of drugs available on the market, which are classified according to their mechanism of

action Inhibitors of acetyl cholinesterase and NMDA receptor inhibitors have beneficial effects on cognitive, functional, andbehavioral symptoms of the disease, but their role in AD pathogenesis is unknown.

Among the kinases reported in human kinome, CDKs, GSK-3, CK1s, DYRK1A and CLK 1 are involved in the two key molecular features of Alzheimer's disease, production of amyloid-b peptides (extracellular plaques) and hyperphosphorylation of the microtubule-binding protein Tau (intracellular neurofibrillary tangles).[33,34] Consequently, small molecule inhibitors acting on these kinases (CDKs, GSK-3, CK1s, DYRK1A and CLK 1) (GSK-3, CDK5, etc.) could be of great therapeutic value in Alzheimer's disease.
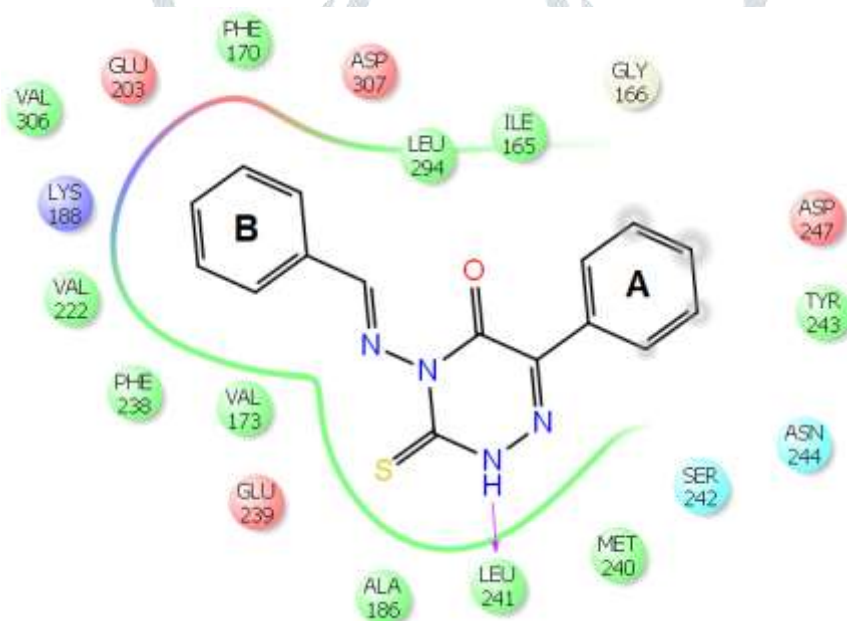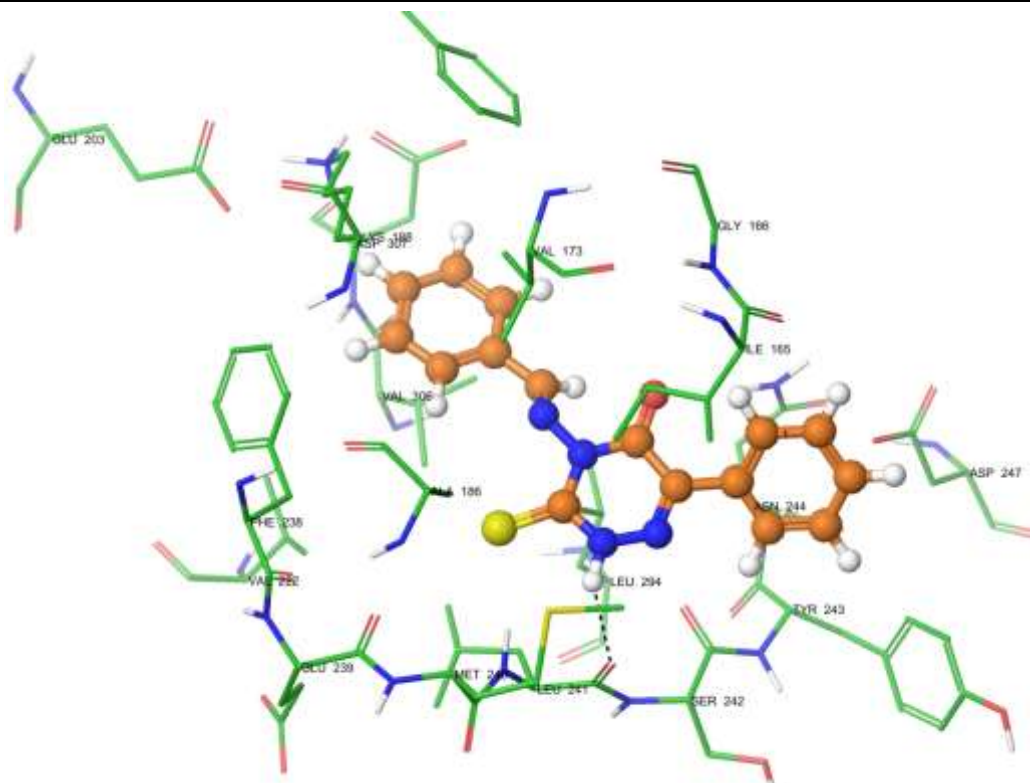
**Discovery of new lead.** A high throughput virtual screening of our inhouse database against crystal structure of DYRK1A (pdb id: 4aze) at computer aided drug design laboratory of our department, led to the identification of a novel lead molecule with drug like properties and good computational affinity towards the DYRK1A.



(*E*)-4-(4-chlorobenzylideneamino)-6-phenyl-3-thioxo-3,4-dihydro-1,2,4-triazin-5(2*H*)-one

*Lead nucleus*

The binding pattern of the lead compound as revealed by docking studies indicated that the molecule binds in ATP binding pocket in a similar binding mode as that of Leucettamine. As shown in figure 4.2 ring (A) the 3-thioxo-3,4-dihydro-1,2,4-triazin-5(2H)-one core of the lead molecule is favourably placed above hinge residues Leu241 and Ala186 forming hydrogen bonding interactions. The phenyl ring A attached to the 3-thioxo-3,4-dihydro-1,2,4-triazin-5(2H)-one is oriented towards solvent exposed cleft of the kinase stabilized by hydrophobic interactions with amino acid residues Ile165, Tyr243 and polar interactions with Asn 244 and Asp247. The phenyl ring B attached to imino bond occupies hydrophobic pocket forming hydrophobic contacts with the aminoacid residues Val 173, Phe238, Val222, Lys188, Val306, Phe170 and Leu294 bordering the pocket.

*Diagrammaticre presentation of Substituted(E)-4-(benzylideneamino)-6-Phenyl-3thioxo*

*1, 2, 4-triazin-5(2H)-one*

*HY- hydrophobic region, HA-hydrogen bond acceptor*

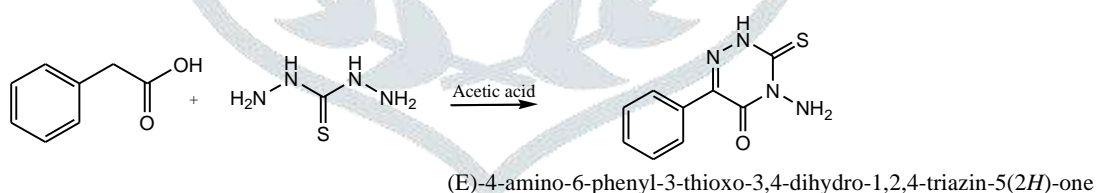## 3. Results and discussion

### 3.1.Chemistry

The 4-(benzylideneamino)-6-    phenyl-3-thioxo-3,4-dihydro -1,2,4-triazin-5(2h)-one (3a–3j) were synthesized in excellent yields by the reaction of 4-chloro-6,7- dimethoxy triazine with aldehyde substrates under the conditions illustrated in Scheme 1. The structures of the synthesized compounds were assigned based on their

elemental analysis and spectral data. For example 1H NMR of 3b shows a singlet for the NH proton at d 11.50 and –OCH3 protons at d = 4.05 and 4.09 (3H for each) and the aromatic protons were observed as three singlets at d = 7.40, 8.86, 8.36 (1H for each singlet) and two doublets at d = 7.59 and 8.08 (with 1H and 2H) and a triplet at d = 7.67 (with 1H) respectively. Similarly, IR Spectra of 3b shows characteristic peaks at 3340 (NH stretching), 3250 (C@N stretching), 3075 (Ar C–H stretching), 1637 (Ar –C–C– stretching), 1280 (–O–CH3 stretch), 1068 (–O– stretching), 784 (–CF3 stretching).

## 3.2 Biological activity

(E)-4-(4-(dimethylamino)benzylideneamino)-6-phenyl-3-thioxo-3,4-dihydro-1,2,4-triazin-5(2H)-one (3a–3j) were tested for their potential inhibitory effect on five different kinases namely CDK5/p25 (CDK5/p25), CK1d/e (casein kinase

1), GSK-3a/b (Glycogen Synthase Kinase 3a/b), DYRK1A (dual-specificity, tyrosine phosphorylation regulated kinase) and CLK1 (cdc2-like kinase 1). All compounds were first tested at a final concentration of 10 lM. Compounds showing less than 50% inhibition were considered as inactive (IC50 >10 lM). Compounds displaying more than 50% inhibition at 10 lM were next tested over a wide range of concentrations (usually 0.01–10 lM) and IC50 values were determined from the dose response curves (Sigma-Plot). The results of the in vitro kinase assay are summarized in Table 1. The results of kinase inhibitory assays demonstrated that none of the synthesized anilino quinazolines showed any inhibitory

activity against CDK5/p25, DYRK1A and CK1d/e at the maximum concentration tested (10 lM). The 4-anilinoquinazolines appeared to be most effective towards CLK1 as four compounds (3a, 3b, 3e and 3h) showed inhibitory activity on the enzyme. Two among the 10 anilinoquinazolines synthesized (compounds 3e and 3h) showed significant inhibitory potency against CLK1 at less than 10 lM concentrations (Fig. 1). It is noteworthy that compound 3e bearing 3, 4 dimethoxy substitution on the aryl ring of the aldehyde.



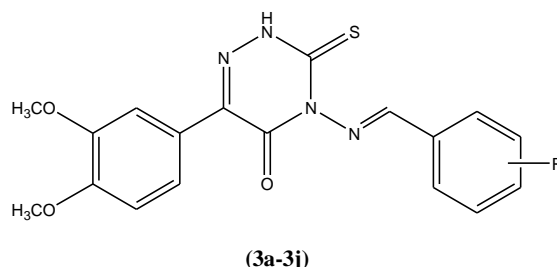(E)-4-amino-6-phenyl-3-thioxo-3,4-dihydro-1,2,4-triazin-5(2H)-one

Reagents and conditions: (i) Isopropanol, 900C, 2-3 hrs

**Scheme 1**. 4-(benzylideneamino)-6- phenyl-3-thioxo-3,4-dihydro -1,2,4-triazin-5(2h)-one **(3a–3j)**.

Table 1
Structural data and kinase inhibitory activity of 4-(benzylideneamino)-6- phenyl-3-thioxo-3,4-dihydro -1,2,4-triazin-5(2h)-one



**(3a-3j)**

| Compound R | | CDK5 | CK1 | CLK1 | DYRK1A rat | GSK3α/β |
|---|---|---|---|---|---|---|
| 3a | 4-(4-(dimethylamino | >10 | >10 | >**10** | >10 | >10 |
| 3b | 3nitrobenzylideneamino | >10 | >10 | >10 | >10 | >10 |
| 3c | 4-(3-chlorobenzylideneamino | >10 | >10 | >10 | >10 | >10 |
| 3d | 4 OH | >10 | >10 | >**10** | >**10** | 3 |
| 3e | 3-4 dimethoxy | >10 | >10 | **2.5** | >10 | >10 |
| 3f | 4 fluro | >10 | >10 | >10 | >10 | >10 |
| 3g | 3,4,5 trimethoxy | >10 | >10 | >10 | >10 | >10 |
| 3h | 4 hydroxy 3,5 dimethoxy | >10 | >10 | >**6.6** | >10 | >10 |
| 3i | 3 hydroxy 4 methoxy | >10 | >10 | >10 | >10 | >10 |
| 3j | 4 chloro | 0.080 | 1.8 | 2.1 | 0.50 | 0.006 |

**Positive control.**

moiety shows less than 5 lM inhibition towards both CLK1 (IC50 = 1.5 lM) and GSK-3a/b (IC50 = 3 lM) enzymes. Surprisingly, compound 3h with 3-fluoro and 4-chloro substitution in the aryl ring exhibited a 5 fold reduced inhibition on CLK1 (IC50 = 7.6 lM) and no inhibition on GSK-3a/b.
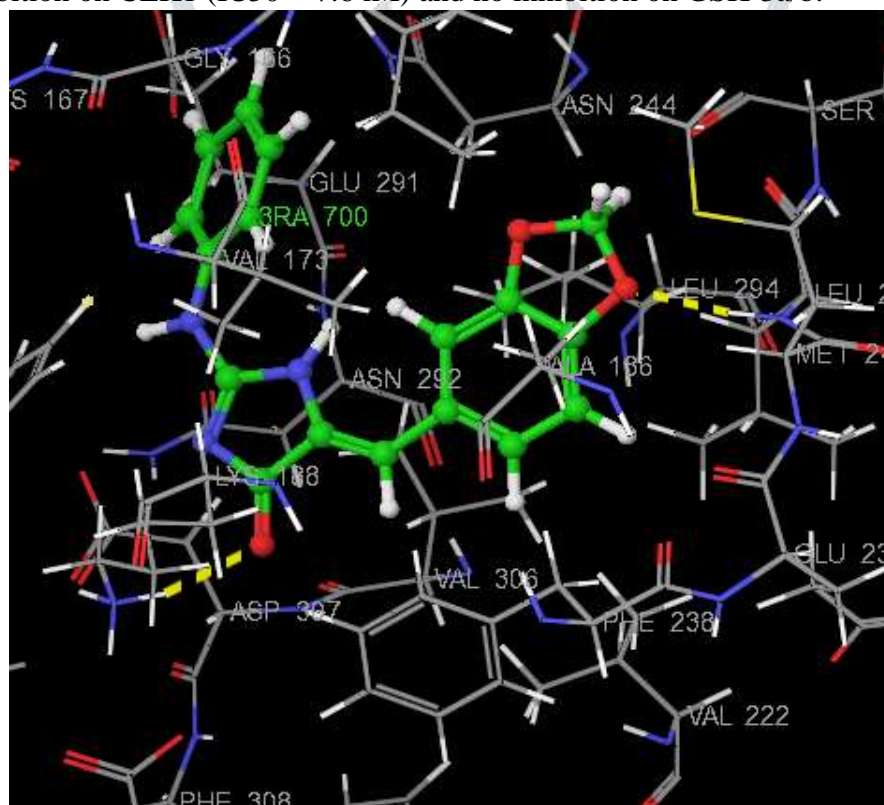


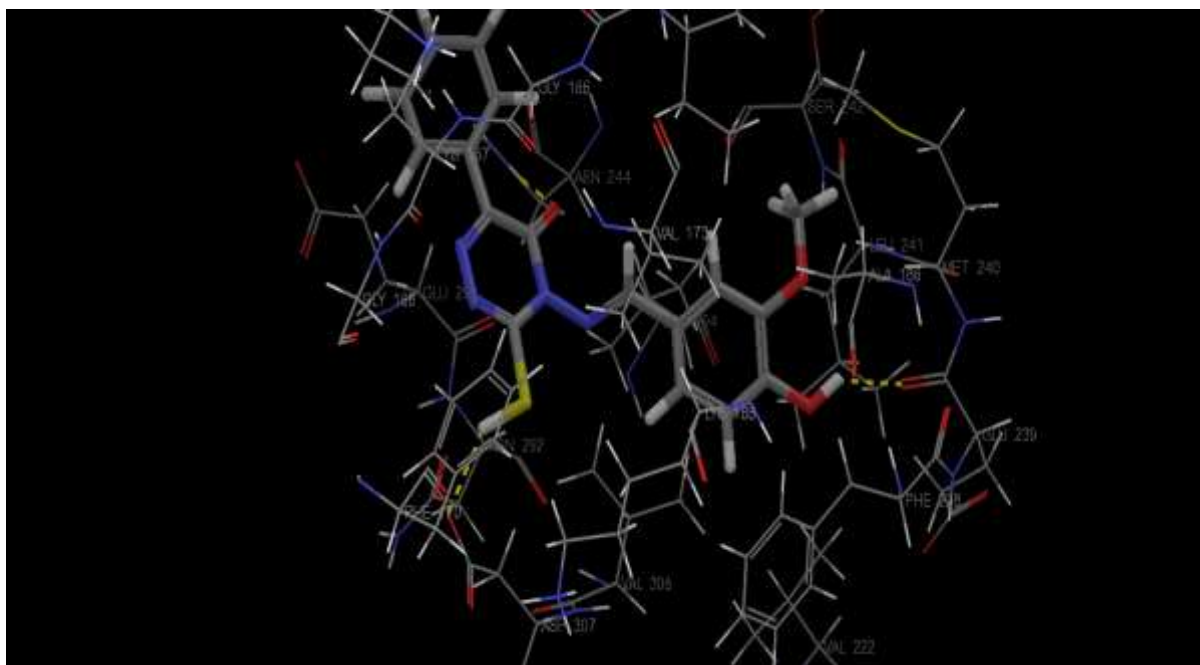*Figure-1     Active Site of DYRK1ABinded with Leucettamine*

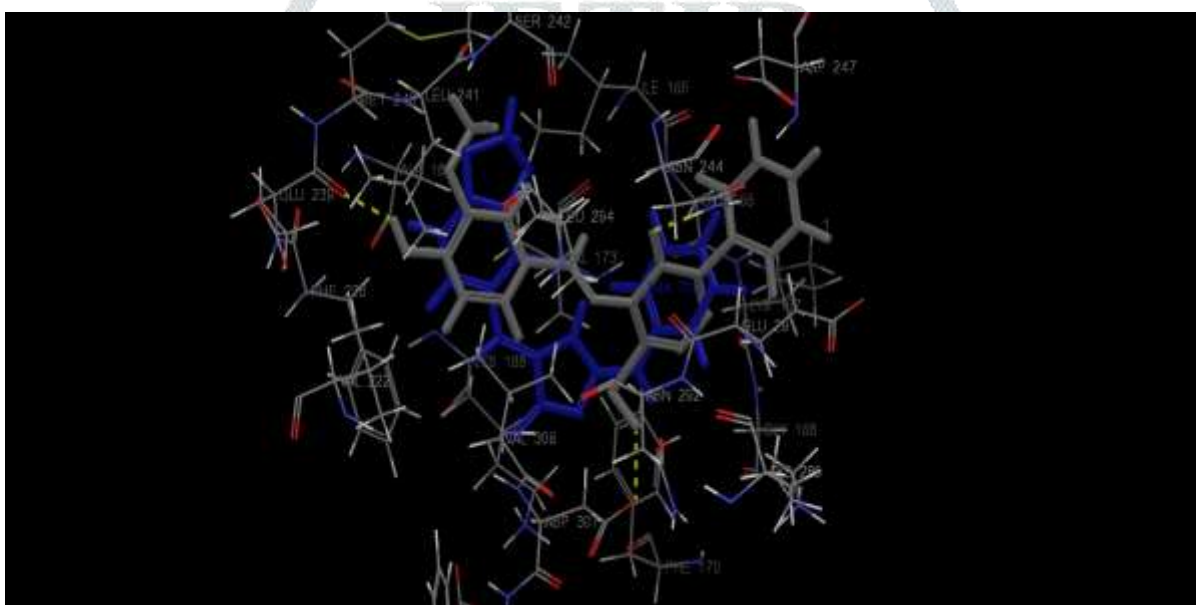*Figure-2 Binding of (highest scoring compound) with DYRK1A*



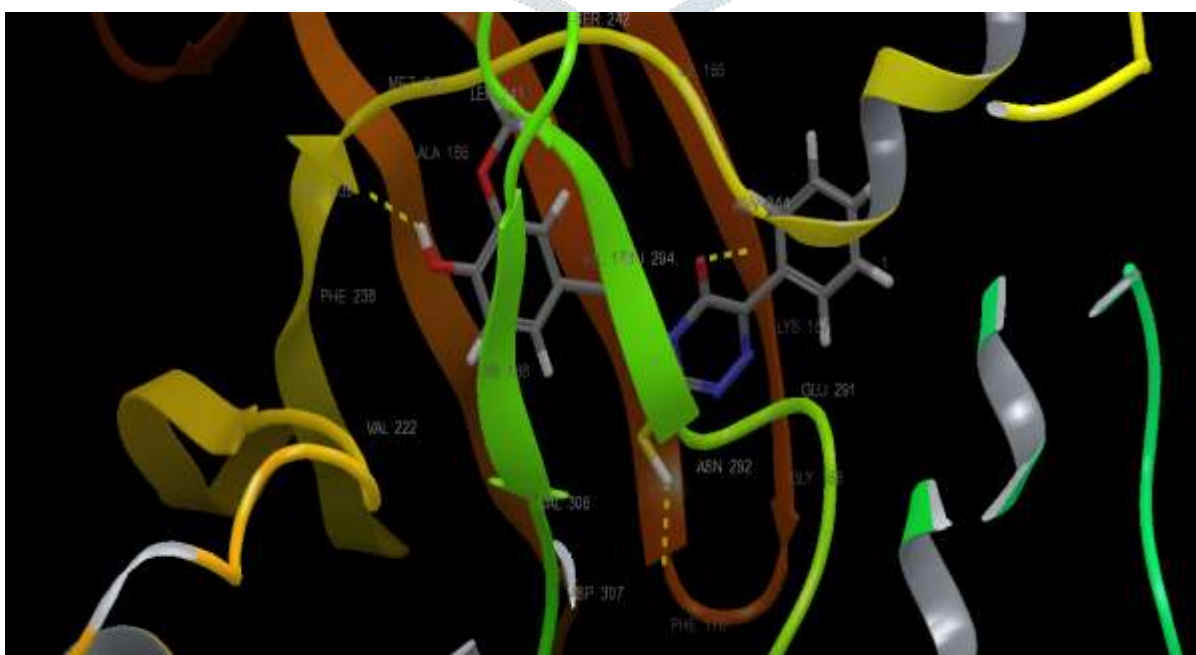*Figure-3 Overlay of Rm-02with reference molecule, Leucettamine(Blue Colour-ref. molecule, Gray Colour*



*Figure-4      Ribbon Structure of DYRKIA with Rm-02*
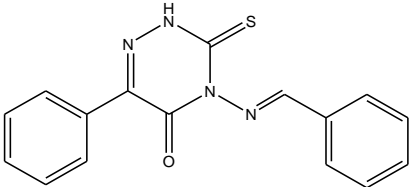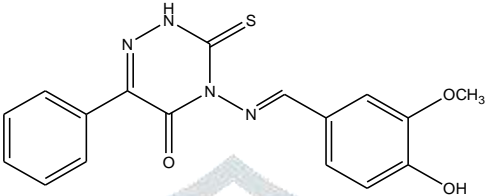
*Figure-5  Hydrophilic Hydrophobic Map of compound Rm14-02with DYRK1A*

## 4.Conclusion

(E)-4-(4-(dimethylamino)benzylideneamino)-6-phenyl-3-thioxo-3,4-dihydro-1,2,4-triazin-5(2H)-one

have emerged as a versatile template for inhibitor design for a diverse range of protein kinases. A series of 4-anilinoquinazolines were synthesized and evaluated for their inhibitory activity against five kinases implicated in Alzheimer's and other neurodegenerative diseases. Two compounds namely 3e and 3h exhibited good potency for CLK1 kinase in comparison to other structurally related kinases like CDK5/p25, CK1d/e and DYRK1A. In addition to potent CLK1 inhibitory activity, compound 3e also showed potent GSK-3a/b inhibition at less than 5 micromolar concentration, making it particularly promising lead for the development of new dual inhibitors of CLK1 and GSK-3a/b kinases. Docking studies were also performed to understand the binding pattern of the active compounds to the CLK1 and GSK-3a/b kinases. The overall findings of this study exemplify the utility of the 4-(benzylideneamino)-6-  phenyl-3-thioxo-3,4-dihydro -1,2,4-triazin-5(2h)-one  scaffold for drug discovery efforts targeted towards kinases related to neurodegenerative diseases. With this understanding, efforts are expended in our laboratory for further optimization of 4-anilinoquinazolines with the hope to develop potent inhibitors of CLK1 and GSK-3a/b kinases with potential therapeutic application in neurodegenerative diseases.

## 5. EXPERIMENTAL

### Docking Analysis

Glide docking uses the assumption of a rigid receptor, although scaling of van der Waals radii of nonpolar atoms, which decreases penalties for close contacts, can be used to model a slight "give" in the receptor and/or ligand. Docking studies of designed compounds were carried out using GLIDE (Grid-based Ligand Docking with Energetics) module version 4.5, Schrödinger, LLC, New York, NY, 2014.The software package running
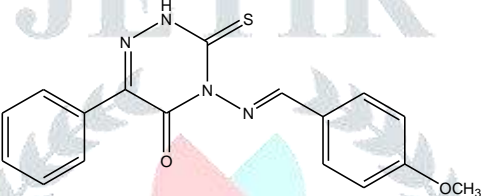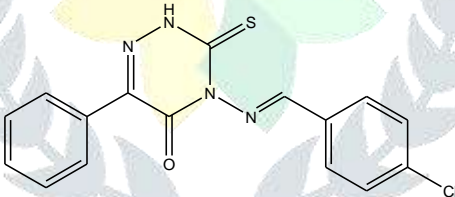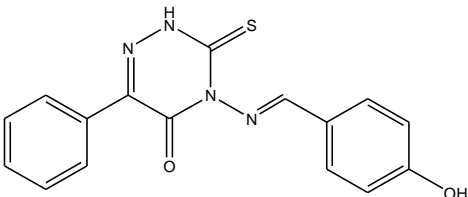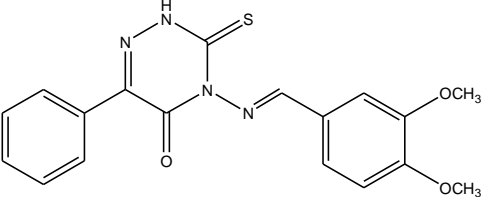
on multi-processor Linux PC.GLIDE has previously been validated & applied successfully to predict the binding orientation of many ligands.

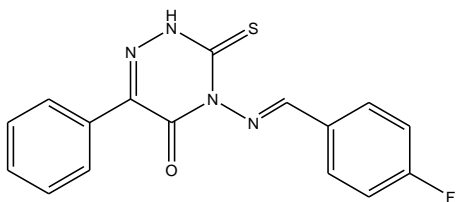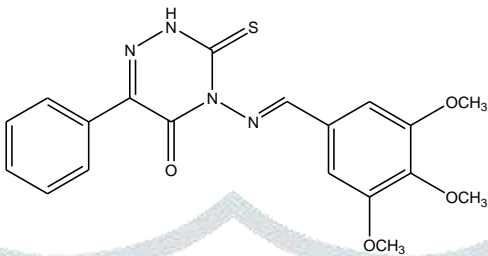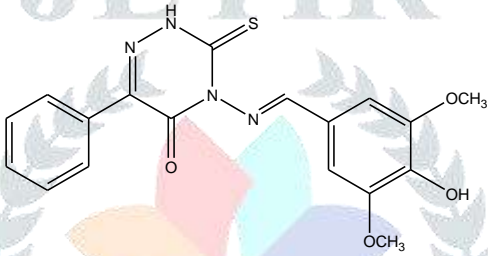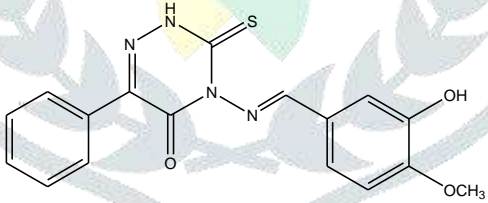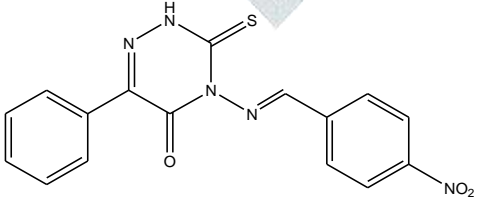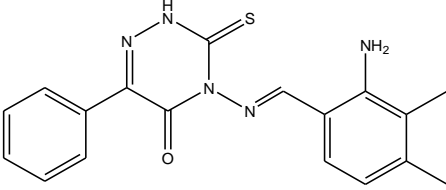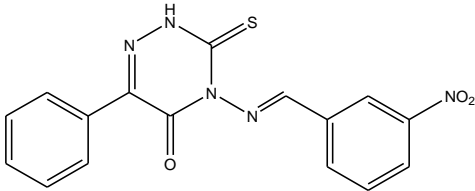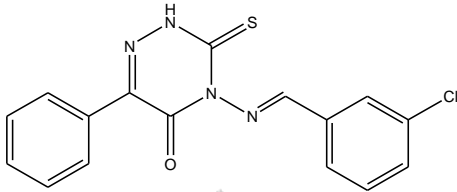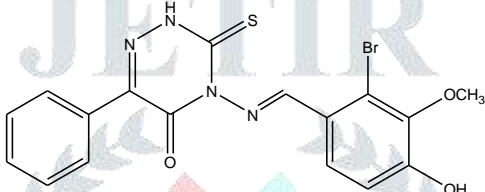The steps involved in docking are as follows:

➢ **Ligand structure**: The chemical structure of each ligand was drawn using build module**.**

➢ **Ligand preparation**: In order to prepare high quality, all-atom 3D structures for large numbers of drug-like molecules, starting with the 3D structures in SD Maestro format, LigPrep was used. LigPrep produced a single, low-energy, 3D structure with corrected chiralities for each successfully processed input structure.

➢ **Preparation of protein**: The typical structure file from the PDB is not suitable for immediate use in molecular modeling calculations. A typical PDB structure file consists only of heavy atoms and may include a co-crystallized ligand, water molecules, metal ions, and cofactors. Some structures are multimeric, and may need to be reduced to a single unit. Because of the limited resolution of X-ray experiments, it can be difficult to distinguish between NH and O, and the placement of these groups must be checked. PDB structures may be missing information on connectivity, which must be assigned, along with bond orders and formal charges. This was done using the Protein Preparation Wizard.

➢ **Receptor Grid Generation**: Receptor grid generation requires a "prepared" structure: an all atom structure with appropriate bond orders and formal charges. Glide searches for favorable interactions between one or more ligand molecules and a receptor molecule, usually a protein. The shape and properties of the receptor are represented on a grid by several different sets of fields that provide progressively more accurate scoring of the ligand poses.

   ➢ **Docking Results**

   ➢ Docking studies of designed compounds were carried out at computer aided drug design (CADD) laboratory by GLIDE (Grid-based Ligand Docking with Energetics, version 4.5, Schrödinger, LLC, New York, NY, 2014) module of Schrödinger software running on multiprocessor-Linux PC. GLIDE has previously been reported for the docking of salicylic acid based receptor with PDB identification code- 1Z57, 3ANQ and was found successfully to predict the binding orientation of many ligands. On the basis of Glide/Docking score of 123 compounds design by isosteric substitution on which 15compound having top score select for synthesis synthesis. The details of their binding pattern at the active site of receptor (1Z57, 3ANQ) were successfully visualized with the help of software. Glide Score is based on ChemScore, but includes a steric-clash term and adds buried polar terms devised by Schrodinger to penalize electrostatic mismatches:

---

➢ Glide Score = 0.065*vdW + 0.130*Coul + Lipo + Hbond + Metal + BuryP + RotB + Site

---

| Sr.No. | Compound Code | Structure | Glide Score |
|--------|---------------|-----------|-------------|
| 1 | RM 14-01 |  | -6.45 |
| 2 | RM 14-02 |  | -8.23 |
| 3 | RM 14-03 |  | -6.96 |
| 4 | RM 14-04 |  | -6.45 |
| 5 | RM 14-05 |  | -7.74 |
| 6 | RM 14-06 |  | -6.45 |

| 7 | RM 14-07 |  | -6.04 |
| 8 | RM 14-08 |  | -6.42 |
| 9 | RM 14-09 |  | -7.24 |
| 10 | RM 14-10 |  | -7.02 |
| 11 | RM 14-11 |  | -6.8 |
| 12 | RM 14-12 |  | -7.0 |

| 13 | RM 14-13 |  | -7.85 |
| 14 | RM 14-14 |  | -7.58 |
| 15 | RM 14-15 |  | -7.28 |

| Sr. No. | Comp. Code | Molecular Formula | Molecular Weight | Colour | Nature |
|---------|-----------|-------------------|------------------|--------|--------|
| 1 | RM14-01 | $C_{16}H_{12}N_4OS$ | 308.07 | yellow | crystalline |
| 2 | RM14-02 | $C_{17}H_{14}N_4O_3S$ | 354.38 | Pale yellow | crystalline |
| 3 | RM14-03 | $C_{17}H_{14}N_4O_2S$ | 338.38 | Pale yellow | crystalline |
| 4 | RM14-04 | $C_{16}H_{11}ClN_4OS$ | 342.8 | Pale yellow | crystalline |
| 5 | RM14-05 | $C_{16}H_{12}N_4O_2S$ | 324.36 | Pale yellow | crystalline |
| 6 | RM14-06 | $C_{18}H_{16}N_4O_3S$ | 368.41 | Dark yellow | crystalline |
| 7 | RM14-07 | $C_{16}H_{11}FN_4OS$ | 326.35 | Pale yellow | crystalline |
| 8 | RM14-08 | $C_{19}H_{18}N_4O_4S$ | 398.44 | Pale yellow | crystalline |
| 9 | RM14-09 | $C_{18}H_{16}N_4O_4S$ | 384.41 | Pale yellow | crystalline |
| 10 | RM14-10 | $C_{17}H_{14}N_4O_3S$ | 354.38 | Pale yellow | crystalline |
| 11 | RM14-11 | $C_{16}H_{11}N_5O_3S$ | 353.36 | Pale yellow | crystalline |

| 12 | RM14-12 | $C_{18}H_{17}N_5OS$ | 351.43 | Pale yellow | crystalline |
| 13 | RM14-13 | $C_{16}H_{11}N_5O_3S$ | 353.36 | Dark yellow | crystalline |
| 14 | RM14-14 | $C_{16}H_{11}ClN_4OS$ | 342.8 | White | crystalline |
| 15 | RM14-15 | $C_{17}H_{13}BrN_4O_3S$ | 433.28 | Pale yellow | crystalline |

**Thin Layer Chromatography (TLC)**

The completion of the reaction was monitored on TLC by using silica gel-G coated plates by using
Petroleum ether: ethyl acetate (7:3) as the eluent and observed in UV light and found $R_f$ values given in table

***Table:-*** *$R_f$ Values, of Synthesized Compounds*

| S. NO. | COMP. CODE | $R_F$ VALUES |
|--------|------------|-------------|
| 1. | RM14-01 | 0.94 |
| 2. | RM14-02 | 0.88 |
| 3. | RM14-03 | 0.82 |
| 4. | RM14-04 | 0.92 |
| 5. | RM14-05 | 0.96 |
| 6. | RM14-06 | 0.90 |
| 7. | RM14-07 | 0.92 |
| 8. | RM14-08 | 0.88 |
| 9. | RM14-09 | 0.92 |
| 10. | RM14-10 | 0.88 |

| 11. | RM14-11 | 0.88 |
|-----|---------|------|
| 12  | RM14-12 | 0.92 |
| 13  | RM14-13 | 0.86 |
| 14  | RM14-14 | 0.65 |
| 15  | RM14-15 | 0.63 |

## Chemistry

All commercial chemicals and solvents used are of reagent grade and were used without further treatment unless otherwise noted. Melting points were determined in open glass capillaries on a Jindal melting point apparatus and were uncorrected. Infrared (IR) spectra were recorded on a Schimadzu FT-IR 8400S infrared spectrophotometer using the ATR accessory. 1H NMR spectra were recorded on a Bruker Avance II 400 spectrometer, using DMSO-d6 as solvent and TMS as internal standard.

**5.2. General procedure for synthesis of 4-(4 chlorobenzylideneamino)-6-   phenyl-3-thioxo-3,4-dihydro -1,2,4-triazin-5(2h)-one (3a–3j)**

A mixture of triazinone (1mmol) the appropriate aldehyde (1mmol) was added followed by glacial acetic acid (1.5ml) and the reaction mixture was refluxed for 2 hr., the reaction to cool to room temperature. The reaction was monitored on TLC by using silica gel-G coated plates by using Chloroform methanol (9:1) as the eluent and observed in UV light. After completion of reaction the Precipitated sold was filtered off and recrystallized from ethanol.

**5.2.1(E)-4-(4-(dimethylamino)benzylideneamino)-6-phenyl-3-thioxo-3,4-dihydro-1,2,4-triazin-5(2H)-**

**one** MP: 170227-229$^0$C, yield (%): 96.20IR $v$ (cm−1): 1523.76(Ar-C=N stretching), 1186.22Ar(C=S) 1701.22(Ar- C=O Stretch), 1591.27(Ar- C=C ring stretching), 2968.45(Ar- CH stretching),. $^1$H NMR (400 MHz, DMSO-$d_6$) δ ppm 3.02 (s, 6 H), 6.79 (d, $J$=9.26 Hz, 2 H) 7.41 - 7.50 (m, 3 H) 7.68 (d, $J$=9.26 Hz, 2 H) 7.87 - 7.93 (m, 2 H) 8.35 (s, 1 H), 13.98 (s, 1 H).

**5.2.2(E)-4-(3-nitrobenzylideneamino)-6-phenyl-3-thioxo-3,4-dihydro-1,2,4-triazin-5(2H)-one**MP:   242-244$^0$C, yield (%):68.74 IR $v$ (cm−1): 1442.75(C-NO2),1182.36 Ar(C=S) 1564.27(Ar- C=N stretching), 1623.13(Ar- C=O Stretch), 1693.50(Ar- C=C ring stretching), 2980.02(Ar- CH stretching),.

$^1$H NMR (400 MHz, DMSO-$d_6$) δ ppm 7.42 - 7.52 (m, 3 H), 7.83 - 7.96 (m, 3 H), 8.36 (d, $J$=8.00 Hz, 1 H), 8.44 - 8.51 (m, 1 H), 8.68 - 8.75 (m, 1 H), 8.92 (s, 1 H), 14.14 (s, 1 H).

**5.2.3(E)-4-(3-chlorobenzylideneamino)-6-phenyl-3-thioxo-3,4-dihydro-1,2,4-triazin-5(2H)-one**MP:   $^0$C, yield (%): 92.75 IR $v$ (cm−1): 721.02(C-Cl) 1575.84,1192.02, (Ar- C=N stretching), 1683.86(Ar- C=O Stretch), 1591.27(Ar- C=C ring stretching), 2962.66(Ar- CH stretching). $^1$H NMR (400 MHz, DMSO-$d_6$) δ ppm 7.44 - 7.48 (m, 3 H) 7.61 (t, $J$=7.88 Hz, 1 H) 7.72 (ddd, $J$=8.00, 2.25, 1.00 Hz, 1 H) 7.86 - 7.94 (m, 3 H) 7.96 (t, $J$=1.88 Hz, 1 H) 8.73 (s, 1 H) 14.10 (s, 1 H).

**5.2.4(E)-4-(4-hydroxybenzylideneamino)-6-phenyl-3-thioxo-3,4-dihydro-1,2,4-triazin-5(2H)-one**MP: 245-247, yield (%):72.95 IR $v$ (cm−1): 1597.06(Ar-C=N stretching),1186.22 Ar(C=S) 1678.07(Ar-C=O Stretch), 1597.06(Ar-C=C ring stretching), 2951.09(Ar-CH stretching), 3379.29(C-OH Stretch). ^{1}H NMR (400 MHz, DMSO-$d_6$) δ ppm 6.91 (d, $J$=8.50 Hz, 2 H) 7.38 - 7.49 (m, 3 H) 7.74 (d, $J$=8.76 Hz, 2 H) 7.85 - 7.95 (m, 2 H) 8.47 (s, 1 H) 10.40 (s, 1 H) 14.02 (s, 1 H).

**5.2.5(E)-4-(3,4-dimethoxybenzylideneamino)-6-phenyl-3-thioxo-3,4-dihydro-1,2,4-triazin-5(2H)-one**MP: 208-210, yield (%):87.95IR $v$ (cm−1): 1510.06(Ar-C=N stretching),1186.22 Ar(C=S)1697.36(Ar-C=O Stretch), 1575.84(Ar-C=C ring stretching), 2920.23(Ar-c CH stretching), 1138.00(C-OCH3 Stretch).^{1}H NMR (400 MHz, DMSO-$d_6$) δ ppm 3.81 (s, 3 H) 3.84 (s, 3 H) 7.12 (d, $J$=8.50 Hz, 1 H) 7.39 - 7.47 (m, 4 H) 7.50 (d, $J$=2.00 Hz, 1 H) 7.87 - 7.94 (m, 2 H) 8.53 (s, 1 H) 14.04 (s, 1 H).

**5.2.6(E)-4-(4-fluorobenzylideneamino)-6-phenyl-3-thioxo-3,4-dihydro-1,2,4-triazin-5(2H)-one**MP: 19240-242, yield (%): 59.17 IR $v$ (cm−1): 933.5(C-Cl Stretching) 1184.29Ar(C=S), 1598.99(Ar-C=N stretching), 1683.86(Ar-C=O Stretch), 1598.06(Ar- C=C ring stretching), 2949.09(Ar- CH stretching). ^{1}H NMR (400 MHz, DMSO-$d_6$) δ ppm 7.38 - 7.47 (m, 5 H) 7.89 - 7.93 (m, 2 H) 8.00 (dd, $J$=9.01, 5.50 Hz, 2 H) 8.70 (s, 1 H) 14.08 (s, 1 H).

**5.2.7(E)-4-(3,4,5-trimethoxybenzylideneamino)-6-phenyl-3-thioxo-3,4-dihydro-1,2,4-triazin-5(2H)-one**MP: 192-194, yield (%):80.86IR $v$ (cm−1): 997.20(C-OCH3)1612.49,1161.75 Ar(C=S) (Ar- C=N stretching), 1683.86(Ar- C=O Stretch), 1575.74(Ar- C=C ring stretching), 2920.23(Ar-CH stretching),.^{1}H NMR (400 MHz, DMSO-$d_6$) δ ppm 3.74 (s, 3 H), 3.83 (s, 6 H), 7.23 (s, 2 H) 7.44 - 7.47 (m, 3 H) 7.89 - 7.93 (m, 2 H) 8.56 (s, 1 H) 14.07 (s, 1 H).

**5.2.8(E)-4-(4-hydroxy-3,5-dimethoxybenzylideneamino)-6-phenyl-3-thioxo-3,4-dihydro-1,2,4-triazin-5(2H)-one** MP: 220-222, yield (%):84.42IR $v$ (cm−1): 1103.28(C-OCH3)1180.00 Ar(C=S)1656.85(Ar- C=N stretching), 1689.64(Ar- C=O Stretch), 1620.00(Ar- C=C ring stretching), 3255.84(Ar- CH stretching),.: ^{1}H NMR (400 MHz, DMSO-$d_6$) δ ppm), 3.81 (s, 6 H), 7.18 (s, 2 H) 7.41 - 7.51 (m, 3 H) 7.87 - 7.97 (m, 2 H) 8.45 (s, 1 H) 9.42 (s, 1 H), 14.06 (s, 1 H).

**5.2.9(E)-4-(3-hydroxy-4-methoxybenzylideneamino)-6-phenyl-3-thioxo-3,4-dihydro-1,2,4-triazin-5(2H)-one**MP: 215-217[0]C, yield (%):82.48 IR $v$ (cm−1): 1118.71(C-OCH3),1170.79 Ar(C=S)1560.06(Ar-C=N stretching), 1699.29(Ar- C=O Stretch), 1597.74(Ar- C=C ring stretching), 2970.38(Ar- CH stretching), 3493.09(C-OH).^{1}H NMR (400 MHz, DMSO-$d_6$) δ ppm 3.84 (s, 3 H), 7.06 (d, $J$=8.25 Hz, 1 H) 7.23 (dd, $J$=8.38, 2.13 Hz, 1 H) 7.41 - 7.48 (m, 4 H) 7.87 - 7.93 (m, 2 H) 8.45 (s, 1 H) 9.54 (s, 1 H) 14.03 (s, 1 H)

**5.2.10(E)-4-(4-nitrobenzylideneamino)-6-phenyl-3-thioxo-3,4-dihydro-1,2,4-triazin-5(2H)-one**MP: 248-250[0]C, yield (%): 87.36 IR $v$ (cm−1): 1411.89(C-NO2),1180 Ar(C=S)1622.13(Ar-C=N stretching), 1699.29 (Ar- C=O Stretch), 1595.13(Ar- C=C ring stretching), 2960.02(Ar- CH stretching),. ^{1}H NMR (400 MHz, DMSO-$d_6$) δ ppm 7.43 - 7.49 (m, 3 H) 7.88 - 7.93 (m, 2 H) 8.17 - 8.21 (m, 2 H) 8.37 - 8.42 (m, 2 H) 8.92 (s, 1 H) 14.14 (s, 1 H).

**5.3.1.2**. Kinase preparations and assays. Kinase activities were assayed in triplicates in buffer A or B, for 30 min at 30 _C, at a final adenosine triphosphate (ATP) concentration of 15 lM. Blank values were subtracted and activities expressed in % of the maximal activity, that is, in the absence of inhibitors. Controls were

performed with appropriate dilutions of dimethylsulfoxide (DMSO). 6 bromoindirubin-30-monoxime (6BIO), a potent inhibitor of several kinases was used as positive control. IC50 values were

calculated from dose–response curves established by Sigma-Plots. The GSK-3, CK1, DYRK1A and CLK1 peptide substrates were obtained from Proteogenix (Oberhausbergen, France).

**5.3.1.2.1**. CDK5/p25. CDK5/p25 (Human, recombinant) was prepared as previously described. Its kinase activity was assayed in buffer A, with 1 mg of histone H1/mL, in the presence of 15 lM [c_33 P] ATP (3000 Ci/mmol; 10 mCi/mL) in a final volume of 30 lL. After 30 min incubation at 30 _C, 25 lL aliquots of supernatant

were spotted onto sheets of Whatman P81 phosphocellulose paper, and 20 s later, the filters were washed eight times (for at least 5 min each time) in a solution of 10 mL phosphoric acid/L of water. The wet filters were counted in the presence of 1 mL ACS (Amersham) scintillation fluid.

**5.3.1.2.2.** GSK-3a/b. GSK-3a/b (Porcine brain, native) was assayed, as described for CDK5/p25 but in buffer A and using a GSK-3 specific substrate (GS-1: YRRAAVPPSPSLSRHSSPHQpSEDEEE) (pS stands for phosphorylated serine).

**5.3.1.2.3**. CK1d/e. CK1d/e (Porcine brain, native) was assayed as described for CDK5/p25 but using the CK1-specific peptide substrate RRKHAAIGpSAYSITA.

**5.3.1.2.4.** DYRK1A. DYRK1A (Rat, recombinant, expressed in Escherichia coli as a glutathione transferase (GST) fusion protein) was purified by affinity chromatography on glutathione agarose and assayed, as described for CDK5/p25 using Woodtide

(KKISGRL-SPIMTEQ) (1.5 lg/assay) as a substrate.

**5.3.1.2.5.** CLK1. CLK1 (Human, recombinant, expressed in E. Coli as GST fusion protein) was assayed in buffer A (+0.15 mg BSA/mL) with RS peptide (GRSRSRSRSRSR) (1 lg/assay).

## 5.3. Induced fit docking

In order to consider the flexibility of both the protein and ligandin the docking experiments, the Induced Fit Docking (IFD) workflow as implemented in the Schrodinger modelling software was used. A detailed account of the theory behind this method can be found elsewhere. The binding site for IFD experiment

was defined by the receptor grid generation. For this we defined the grid centered at the bound ligand utilizing the automatic box size option (meaning that the program automatically determine the size of the box according to the size of the bound ligand). During the IFD workflow, the ligands were initially docked into the receptor using the Glide program with the van der Waals radii scaling of 0.5 for the both the ligands and the receptor. Furthermore, A maximum of 20 top poses for each of the ligands were retained for protein flexibility sampling using the the Prime module of the Schrodinger software. Residues within 5 A from

the ligands in any of the top poses were included for conformation search and energy minimization and the complexes (receptor– ligand conformations) which have energy of <30 kcal/mol were considered for the re-docking step using the extra precision (XP) mode in the Glide program.

## Acknowledgments

## References

1. Hanger, D. P.; Anderton, B. H.; Noble, W. Trends Mol. Med. 2009, 15, 112.

2. Meijer, L.; Flajolet, M.; Greengard, P. Trends Pharmacol. Sci. 2004, 25, 471.

3. Polychronopoulos, P.; Magiatis, P.; Skaltsounis, A. L.; Myrianthopoulos, V.; Mikros, E.; Tarricone, A.; Musacchio, A.; Roe, S. M.; Pearl, L.; Leost, M.; Greengard, P.; Meijer, L. J. Med. Chem. 2004, 47, 935.

4. Cohen, P. Eur. J. Biochem. 2001, 268, 5001.

5. Cohen, P. Nat. Rev. Drug Disc. 2002, 1, 309.

6. Perl, D. P. Mt. Sinai J. Med. 2010, 77, 32.

7. Trinczek, B.; Biernat, J.; Baumann, K.; Mandelkow, E. M.; Mandelkow, E. Mol. Biol. Cell 1995, 6, 1887.

8. Smith, B.; Medda, F.; Gokhale, V.; Dunckley, T.; Hulme, C. ACS Chem. Neurosci. 2012, 3, 857.

9. Arriagada, P. V.; Growdon, J. H.; Hedley-Whyte, E. T.; Hyman, B. T. Neurology 1992, 42, 631.

10. Churcher, I. Curr. Top. Med. Chem. 2006, 6, 579.

11. Martin, L.; Latypova, X.; Wilson, C. M.; Magnaudeix, A.; Perrin, M.-L.; Yardin, C.;Terro, F. Ageing Res. Rev. 2013, 12, 289.

12. Flight, M. H. Nat. Rev. Drug Disc. 2013, 12, 739.

13. Hartmann, A. M.; Rujescu, D.; Giannakouros, T.; Nikolakaki, E.; Goedert, M.; Mandelkow, E. M.; Gao, Q. S.; Andreadis, A.; Stamm, S. Mol. Cell. Neurosci. 2001, 18, 80.

14. Wang, D.; Gao, F. Chem. Cent. J. 2013, 7, 95.

15. Marzaro, G.; Guiotto, A.; Chilin, A. Exp. Opin. Ther. Pat. 2012, 22, 223.

16. Alafeefy, A. M.; Kadi, A. A.; Al-Deeb, O. A.; El-Tahir, K. E.; Al-Jaber, N. A. Eur. J. Med. Chem. 2010, 45, 4947.

17. Gineinah, M. M.; El-Sherbeny, M. A.; Nasr, M. N.; Maarouf, A. R. Arch. Pharm. 2002, 335, 556.

18. Rather, B. A.; Raj, T.; Reddy, A.; Ishar, M. P.; Sivakumar, S.; Paneerselvam, P. Arch. Pharm. 2010, 343, 108.

19. Lew, J.; Qi, Z.; Huang, Q.Q.; Paudel, H.; Matsuura, I.; Matsushita, M.; Zhu, X.; Wang, J.H. Structure, function, and regulation of neuronal Cdc2-like protein kinase. *Neurobiol Aging.* **1995**, *16(3)*, 263-8.

20. Moeslein FM, Myers MP, Landreth GE, The CLK family kinase, CLK1 and CLK2, phosphorylate and activate the tyrosine phosphate PTP-1B J Biol Chem 1999, 274(38), 26697-704.

21. www.uniprot.org

22. Martin L.; Latypova X.; Wilson C.M.; Magnaudeix A.; Perrin M.; Yardin C.;Terro F. Tau protein kinases: Involvement in Alzheimer's disease. *Ageing Research Reviews.***2012**,6

23. Rosenthal, A.S.; Tanega, C.; Shen, M.; Mott, B.T.; Bougie, J.M.; Nguyen, D.T.; Misteli, T.; Auld, D.S.; Maloney, D.J.; Thomas, C.J. Potent and selective small molecule inhibitors of specific isoforms of Cdc2-like kinases (Clk) and dual specificity tyrosine-phosphorylation-regulated kinases (Dyrk). *Bioorg Med Chem Lett*. **2011**, *21*, 3152-8.

24. Mott, B.T.; Tanega, C.; Shen, M.; Maloney, D.J.; Shinn, P.; Leister, W.; Marugan, J.J.; Inglese, J.; Austin, C.P.; Misteli, T.; Auld, D.S.; Thomas, C.J. Evaluation of substituted 6-arylquinazolin-4-amines as potent and selective inhibitors of cdc2-like kinases (Clk). *Bioorg Med Chem Lett*. **2009**, *19*, 6700-5.

25. Ogawa, Y.; Hagiwara, M. Challenges to congenital genetic disorders with "RNA-targeting" chemical compounds. *Pharmacol Ther*. **2012**.

26. Nguyen, T.B.; Lozach, O.; Surpateanu, G.; Wang, Q.; Retailleau, P.; Iorga, B.I.; Meijer, L.; Guéritte, F. Synthesis, Biological Evaluation and Molecular Modeling of Natural and Unnatural Flavonoidal Alkaloids, Inhibitors of Kinases. *J Med Chem*. **2012**, *55(6),* 2811-9.

27. Cuny, G.D.; Ulyanova, N.P.; Patnaik, D.; Liu, J.F.; Lin, X.; Auerbach, K.; Ray, S.S.; Xian, J.; Glicksman, M.A.; Stein, R.L.; Higgins, J.M. Structure-activity relationship study of beta-carboline derivatives as haspin kinase inhibitors. *Bioorg Med Chem Lett*. **2012**, *22*, 2015-9.

28. Coffman, K.; Brodney, M.; Cook, J.; Lanyon, L.; Pandit, J.; Sakya, S.; Schachter, J.; Tseng-Lovering, E.; Wessel, M. 6-Amino-4-(pyrimidin-4-yl)pyridones: Novel glycogen synthase kinase-3b inhibitors. *Bioorg Med Chem Lett*. **2011**,*21*,1429-33

29. Huber, K.; Brault, L.; Fedorov, O.; Gasser, C.; Filippakopoulos, P.; Bullock, A.N.; Fabbro, D.; Trappe, J.; Schwaller, J.; Knapp, S.; Bracher, F. 7,8-Dichloro-1-oxo-β-carbolines as a Versatile Scaffold for the Development of Potent and Selective Kinase Inhibitors with Unusual Binding Modes . *J Med Chem*. **2012**, *55*, 403-13.

30. Nguyen, T.B.; Lozach, O.; Surpateanu, G.; Wang, Q.; Retailleau, P.; Iorga, B.I.; Meijer, L.; Guéritte, F. Synthesis, Protein Kinase Inhibitory Potencies and in Vitro Antiproliferative Activities of Meridianin Derivatives. *J Med Chem*. **2011** *54(13):*4474-89.

31. Debdab, M.; Carreaux, F.; Renault, S.; Soundararajan, M.; Fedorov, O.; Filippakopoulos, P.; Lozach, O.; Babault, L.; Tahtouh, T.; Baratte, B.; Ogawa, Y.; Hagiwara, M.; Eisenreich, A.; Rauch, U.; Knapp, S.; Meijer, L.; Bazureau, J.P. Leucettines, a class of potent inhibitors of cdc2-like kinases and dual specificity, tyrosine phosphorylation regulated kinases derived from the marine sponge leucettamine B: modulation of alternative pre-RNA splicing. *J. Med. Chem*. **2011,** *54*, 4172–4186.

32. Krishnamurty, R.; Brock, A.M.; Maly, D.J. Protein kinase affinity reagents based on a 5-aminoindazole scaffold. *Bioorg Med Chem Lett*. **2011**, *21*, 550-4.

33. Fedorov, O.; Huber, K.; Eisenreich, A.; Filippakopoulos, P.; King, O.; Bullock, AN.; Szklarczyk, D.; Jensen, L.J.; Fabbro, D.; Trappe, J.; Rauch, U.; Bracher, F.; Knapp, S. Specific CLK Inhibitors from a Novel Chemotype for Regulation of Alternative Splicing. *Chem Biol.* **2011**, *18*, 67-76.

34. Wood, J.G.; Lu, Q.; Reich, C.; Zinsmeister, P. Proline-directed kinase systems in Alzheimer's disease pathology. *Neurosci Lett.* **1993,** *156*, 83-6.

35. Nguyen, T.B.; Lozach, O.; Surpateanu, G.; Wang, Q.; Retailleau, P.; Iorga, B.I.; Meijer, L.; Guéritte, F. Synthesis, Protein Kinase Inhibitory Potencies and in Vitro Antiproliferative Activities of Meridianin Derivatives. *J Med*

*Chem*. **2011** *54(13):*4474-89.

36. Sliman, F.; Blairvacq, M.; Durieu, E.; Meijer, L.; Rodrigo, J.; Desmaële, D. Identification and structure-activity relationship of 8-hydroxy-quinoline-7-carboxylic acid derivatives as inhibitors of Pim-1 kinase. *Bioorg Med Chem Lett*. **2010**, *20*, 2801-5.

37. Daniel P. Perl, Neuropathology of Alzheimer's disease. *Mount Sinai Journal of Medicine*, **2010**, 77, 32–42.

38. Liu, F.; Gong, C.X. Tau exon 10 alternative splicing and tauopathies Molecular *Neurodegeneration* **2008**, *3*, 8.

39. Mazanetz MP, Fischer PM, Untangling tau hyperphosphorylation in drug design for neurodegenerative diseases. *Nat Rev Drug Discov.* **2007**, 6(6), 464-79.